Microstructure Development in Calcium Aluminate Cement – Fly Ash Mixes

A. Hidalgo[1], M.C. Alonso[1], J.L. García[1], S. Petit[2], L. Fernández Luco[1], C. Andrade[1]

[1]*Instituto de Ciencias de la Construcción Eduardo Torroja (IETcc-CSIC), Madrid, Spain;* [2] *Université de Poitiers, CNRS UMR 6532 HydrASA, Poitiers Cedex, France*

Abstract

Calcium aluminate cement (CAC) and fly ash (FA) mixes represent an interesting alternative for the stabilization of CAC hydrates, which might be attributed to a microstructure based mainly on aluminosilicates.

This paper deals with the microstructure of cement pastes fabricated with mixtures CAC-FA and its evolution over time. Different techniques as DTA/TGA, XRD and FTIR, have been used to assess the microstructure of combinations of CAC + FA.

The analysis of the results shows that most crystalline phases of hexagonal shape (CAH_{10} and C_2AH_8) have evolved into cubic forms containing silica (type hydrogranet: $C_3AS_{3-X}H_{2X}$). Furthermore, the amount of gibbsite seems to decrease when increasing the % of FA. This suggests that gibbsite would react with blended agents to form new hydrated phases, which could cause the generation of aluminosilicates with undefined composition, although in low %, thus giving a high level of confidence to the hypothesis of CAC hydrates stabilization.

1. Introduction

The most widely identified degradation process suffered by calcium aluminate cement (CAC) is the so called conversion of hexagonal calcium aluminate hydrate to cubic form [1-3], which is unavoidable and irreversible.

This conversion is usually followed by an increase in porosity determined by the different densities of these hydrates and the subsequent loss of strength. Conversion reactions are shown below:

$$3\ CAH_{10} \rightarrow C_3AH_6 + 2\ AH_3 + 18\ H \quad (1)$$

$$3\ C_2AH_8 \rightarrow 2\ C_3AH_6 + AH_3 + 9\ H \quad (2)$$

Being CAH10: $CaAl_2O_{14}H_{2O}$, C_2AH_8: $Ca_2Al_2O_{13}H_{16}$, C_3AH_6: $Ca_3Al_2(OH)_{12}$, AH_3: $Al(OH)_3$, and H: H_2O.

Some cases of degradation of concretes fabricated with calcium aluminate cement (CAC) were registered in Spain over many years [4, 5], although it was not until 1990, when a building collapsed with one fatality, that a social concern was generated.

An interesting way to reduce the hydrate conversion and the decreasing of strength is to replace some of the CAC by blast furnace slag (BFS) or a pozzolan such as microsilica and metakaolin [6-9]. Majumdar showed that with concrete based on equal amounts of CAC and BFS cured at either 20ºC or 38ºC, the compressive strength increased continuously over a period of one year, in contrast to control samples made without any BFS content, which showed decreases in strength associated with conversion. These concretes have also shown good chemical resistance and reduced temperature rise on curing [10, 11].

The reaction that avoids the conversion process could be produced in the following way [5, 11-13]: the silica content of the mineral addition would react with the calcium aluminates, initially avoiding the formation of C_2AH_8 and, subsequently the conversion in C_3AH_6. Therefore, instead this cubic phase, a hexagonal hydrated called strätlingite or gehlenite ($Ca_2Al_2SiO_7 \cdot 8H_2O$; C_2ASH_8) is formed. Majumdar et al. [7] considered that the amount of C_2ASH_8 is dependent on the capacity of a mineral addition to release silica.

Studies about stabilisation of CAC with BFS or silica fume (SF) are scarce. The reaction of CAC with fly ash (FA) has been analysed by Collepardi et al. [12] indicating as conclusion of the study that FA is not suitable for reducing the transformation of hexagonal hydrates into the cubic phases.

The aim of this work was the evaluation of microstructural changes produced in calcium aluminate cements blended with fly ash. Medium Infrared spectroscopy (FTIR), thermal analysis (DTA/TGA), and X Ray diffraction (XRD), were used to characterize the microstructural evolution of the fabricated cement pastes.

2. Experimental

2.1 Materials

Spanish calcium aluminate cement (supplied by Cementos Molins, Sant Vicenç dels Horts, Barcelona, Spain) and fly ash (supplied by Cia. Valenciana de Cementos Pórtland S.A, Alcalá de Guadaira, Seville,

Spain) were used for the testing program. Fly ash was classified as Class F according to the ASTM definition. Chemical composition of raw materials is presented in Table 1.

Table 1. Chemical composition of CAC and FA.

	LI	IR	SiO_2	Al_2O_3	Fe_2O_3	CaO (total)	MgO	SO_3	Na_2O	K_2O	CaO (free)
CAC	0.43	2.31	2.60	45.29	14.66	36.9	0.71	-	0.15	0.1	0.11
FA	2.24	0.53	55.63	27.92	5.51	4.63	2.3	-	0.63	3.25	0.15

LI: lost of ignition; IR: insoluble residue.

Cement pastes were fabricated with a water/binder=0.5, being their formulations 100%CAC (CF-1), 70%CAC+30%FA (CF-2) and 50%CAC+50%FA (CF-3). Demineralised water was used for mixes, whose were hydrated in sealed conditions (98% relative humidity and 20±2ºC). Hydration was stopped at 2, 7, 30 and 90 days; then cement pastes were grounded to a powder with particle size lower than 75 μm and the process of hydration was interrupted in each case by “freezing” the sample with ethanol and acetone.

X ray diffraction analysis of the fly ash (not shown) indicated that it was mainly composed of mullite, quartz, magnetite, CaO, calcite and glassy phases.

2.2 Methods

The evolution of the main crystalline phases of the cement pastes during hydration was determined by means of thermal analysis (DTA/TGA), X-Ray diffraction (XRD) and medium infrared spectroscopy (FTIR).

DTA/TGA data have been obtained from a DTA/TG SEIKO 320U thermal analyzer with a resolution of 0.01 mg. The sample was taken in a platinum crucible and heated from room temperature to 1200 ºC at a heating rate of 10°C/min using nitrogen as a medium under static condition. Alumina powder was used as the reference material.

Cement pastes were analyzed by X-ray diffraction (XRD) from a 2θ value of 5 to 60º with a Philips PW1710 instrument using a step of 0.02º and Cu$K\alpha_1$ radiation.

Medium infrared spectra were taken at room temperature with a Fourier transform IR spectrometer (FTIR) equipped with a DTGS detector and a CsI beam splitter. For each sample, 256 scans were recorded in the 4000-250 cm^{-1} spectral range with a resolution of 4 cm^{-1}. Test samples were prepared by mixing cement pastes with potassium bromide in an agate

mortar, fabricating the 12 mm diameter dried KBr pellets (0.15 mg of sample and 150 mg of KBr).

3. Results and discussion

3.1 Thermal analysis, DTA/TGA

The identification of mineral components for mixes CAC-FA, and their quantification, using DTA/TGA is difficult and often may be impossible due to overlapping of dehydration and decarbonation processes of different solid phases; however an estimation of the mineral content can be made in some cases. Calculations for some solid phases are presented in Table 2. Figure 1 shows the differential thermal analysis, DTA curves, for the three formulations, at 2, 7, and 30 reaction times.

The major endothermic effects recorded afterwards can be attributed to dehydration of $Al_2O_3 \cdot xH_2O$, CAH_{10}, C_2AH_8, AH_3 and carbonates.

The initial step in the thermal decomposition of samples is the endothermic effect at ~90ºC, which is induced by $Al_2O_3 \cdot xH_2O$ (figure 1). The loss of weight related with this endothermic effect increases with the introduction of fly ash in the paste formulation (see Table 2), indicating that an amorphous aluminium hydroxide is produced as a product formed in the hydration reaction of calcium aluminates and fly ash. However, the broadening of endotherms at the temperature range from 60–120ºC in samples including fly ash indicates the presence of a higher amount of combined water associated with increased quantity of this phase and other hydrated minerals.

Table 2. % of solid phases in mixes after 2, 7, 30and 90 days

Sample	CF-1				CF-2				CF-3			
Days	2	7	30	90	2	7	30	90	2	7	30	90
$Al_2O_3 \cdot xH_2O$ (80-120ºC) [14, 15]	1	0.5	1.2	0.4	2.19	1.35	1.75	0.48	2.36	1.70	1.94	1.06
CAH_{10} - C_2AH_8 (120-200ºC) [15-17]	1.19	0.98	0.96	0.70	4.99	5.29	4.79	1.12	5.25	4.82	4.50	1.98
AH_3 (220-280ºC) [14, 15]	6.67	7.09	9.18	7.73	6.20	6.72	5.56	5.23	3.24	3.73	3.16	3.96
C_3AH_6 or $C_3AS_{3-X}H_{2X}$ (280-350ºC) [15, 17]	8.01	6.99	3.91	5.28	1.60	1.13	1.41	6.62	0.91	0.84	0.85	5.36
Carbonates (660-725ºC) [14]	0.32	1.29	4.40	6.39	0.19	0.69	2.44	1.05	0.16	0.53	2.31	1.19

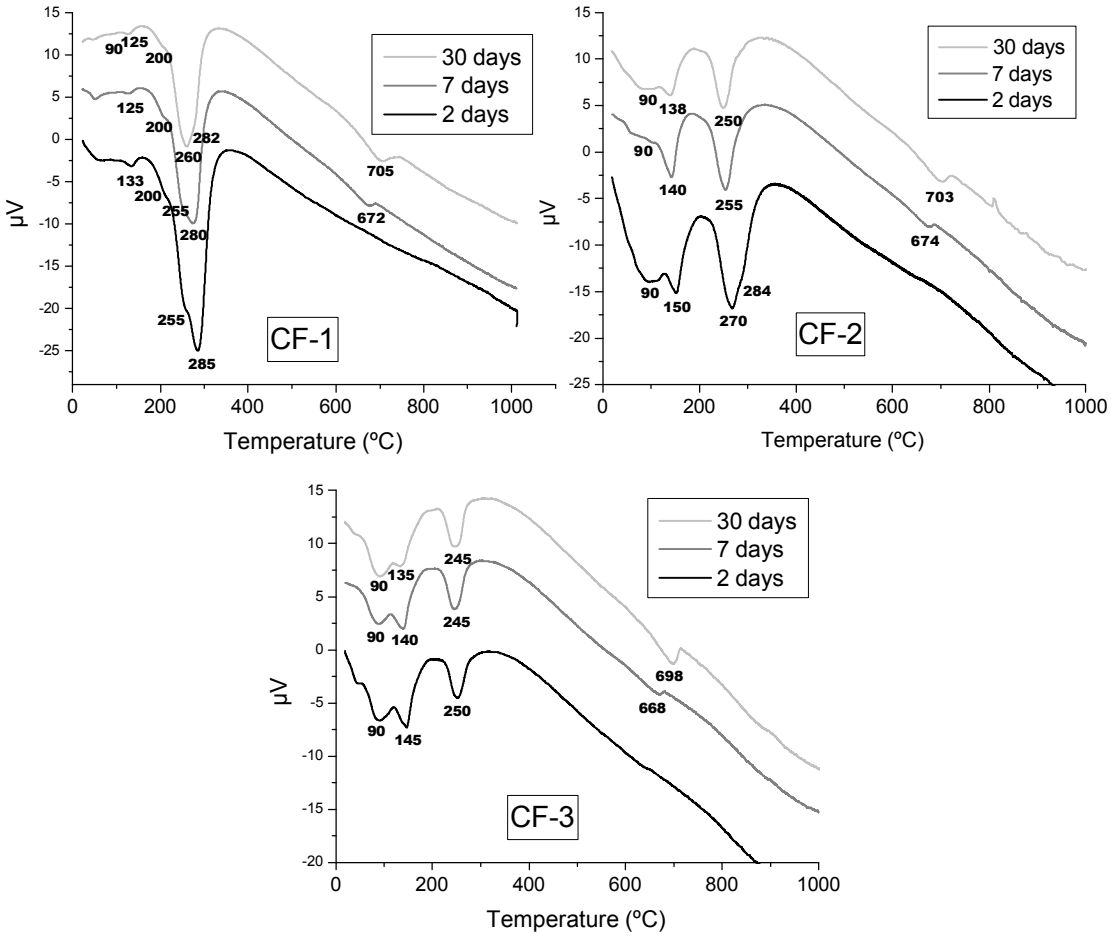

Figure 1. DTAs of cement pastes at 2, 7 and 30 days of hydration.

The endotherm around 140ºC is attributed to the dehydration of hexagonal calcium aluminate hydrates, i.e. CAH_{10} and C_2AH_8. The content of hexagonal hydrates is higher for formulations including fly ash on their composition, as can be seen in Table 2 and figure 1, fact that can be related with the deceleration of the conversion reaction. Additionally these samples including fly ash on their compositions show a decrease on the hexagonal hydrate content with time, while the content of a member of the grossular-hydrogrossular solid reaction ($C_3AS_{3-X}H_{2X}$) increases, as can be observed in table 2.

Endothermic peaks in the range 280-350ºC indicate the presence of a member of the hydrogarnet series, $C_3AS_{3-x}H_{2x}$, with x: 0 to 3 (hydrogarnet). The introduction of silica in the structure of hydrogranet, C_3AH_6, and the subsequent decrease in the crystallization water could

produce a displacement of the endothermic effect and the overlapping with that one of gibbsite. This can be the reason for the presence of one peak centred at 250ºC for the samples including fly ash, instead of the two ones in the range 250-290ºC that appear in CF-1 sample.

In all samples gibbsite shows endotherms at 220-280ºC. Gibbsite content decreases with the increase on fly ash content on formulations (see table 2). The decrease in gibbsite content can be related with the elimination of conversion reactions (1) and (2).

In general, carbonates show peaks at the temperature range of 625-875ºC. In the 2 and 7 days hydrated samples, the decarbonation occurred at lower temperature (the peak temperature was ≈670ºC). This fact can be related with the presence of different types of carbonates, different content or different crystallinity degree.

3.2 XRD

Some authors [13] reported that in the system CAC-SF, silica reacts with the calcium aluminate phases in the cement and water to form different crystalline hydrates (with variable proportions of Ca, Al, Si) such as $Ca_2Al_2SiO_7 \cdot 8H_2O$ (C_2ASH_8; strätlingite), $Ca_3Al_2(SiO_4)_{3-x}(OH)_{4x}$ ($0<x<3$) (katoite) and not very well defined and complex zeolite-type phases.

Table 3 shows the crystalline phases present in the samples object of this study. After 90 days hydration, the main component of pastes is an aluminosilicate member of the solid solution grossular (C_3AS_3)-hydrogrossular (C_3AH_6) represented in general as $C_3AS_{3-x}H_{2x}$. The influence of an isomorphous replacement in the XRD pattern is well known; a variation of pattern peaks is observed. Due to the Si introduction, it was observed that all samples displayed some differences in diffraction patterns; that is a shift of measured diffraction peaks of C_3AH_6 theoretical ones (ICDD card 24-0217). The shift of diffraction peaks increases with the introduction of Si in the structure.

Table 4 presents the variation of measured diffraction peaks for each samples, respect to the powder diffraction file 24-0217 (ICDD 2000 and ICSD data base) at 90 days of hydration. The variation respect to remaining anhydrous calcium monoaluminate (CA) peaks (diffraction file 34-0440), is also included. This solid phase could be used as internal standard, because it does not show any variation from its theoretical pattern. The shift can be observed in figure 2, which presents the X ray spectra of CF-1 and CF-3 samples at 90 days of hydration.

For all samples, the hexagonal phases, CAH_{10} and C_2AH_8, disappear with time so it is possible to suppose that the hexagonal hydrates are transformed into C_3AH_6 for CF-1 and aluminosilicates for CF-2 and CF-3.

Gibbsite and aluminosilicates, identified as strätlingite (C_2ASH_8; $Ca_2Al_2SiO_7{\cdot}8H_2O$) and laumontite ($CAS_4H_4$; $CaAl_2Si_4O_{12}{\cdot}4H_2O$), are also identified by XRD. The appearance of grossular (C_3AS_3), an end member of the $C_3AS_{3-X}H_{2X}$ solid solution, in the CF-3 sample, indicates that no more solid solution is formed. Then, the reaction between silica from FA and aluminates, produces the neoformation of aluminosilicates such as laumontite (CAS_4H_4) and strätlingite (C_2ASH_8) (see table 3).

Table 3. Crystalline phases of the fabricated pastes at the different reaction times

Sample	CF-1				CF-2				CF-3			
Days	2	7	30	90	2	7	30	90	2	7	30	90
CA	x	x	x	x	xxx	xx	xx	x	xx	xx	x	x
CAH_{10}	x	-	-	-	xx	xx	-	-	xxx	x	-	-
C_2AH_8	x	-	-	-	xx	xx	-	-	xx	xx	-	-
$C_3AS_{3-X}H_{2X}$	x	xxx	xxx	xxx	-	x	xxx	xxx	-	x	xxx	xxx
$C_{12}A_7$	xxx	xxx	xxx	xxx	x	x	x	x	x	x	x	x
C_4AF	x	x	x	x	x	x	x	x	x	x	-	-
AH_3	x	xx	xxx	xxx	x	xx	xx	xx	x	xx	xx	xx
C_2ASH_8	-	-	-	-	-	x	x	x	-	x	xx	xx
CAS_4H_4	-	-	-	-	-	-	-	-	-	-	x	x
C_3AS_3	-	-	-	-	-	-	-	-	-	x	x	x
C_4AcH_{11}	-	-	-	-	x	x	x	-	x	x	x	-
Aragonite	x	x	x	x	x	x	x	x	x	x	x	x
Calcite	x	x	x	x	x	x	x	x	x	x	x	x

x: little content; xx: medium content; xxx: high content. C_3AH_6 is one of the end members of the solid solution $C_3AS_{3-X}H_{2X}$.

Carbonates such us aragonite and calcite were also detected in X ray powder diffraction. Calcium monocarboaluminate hydrate (C_4AcH_{11}) is present at early ages of hydration in the pastes with fly ash.

From table 3 it can be also extracted that calcium aluminate $CaAl_2O_4$ (CA) remains at early ages. Other possible components are $Ca_{12}Al_{14}O_{33}$ ($C_{12}A_7$) and the brownmillerite, $Ca_2Al_{1.1}Fe^{2+}_{0.9}O_5$ (C_4AF).

Table 4. Shift of the measured diffraction peaks with respect to the Powder Diffraction File: 24-0217 (ICDD 2000 and ICSD data base)

Sample	2theta		Difference	2 theta	Difference
	Measured	C_3AH_6 ICDD 24-0217		CA ICDD 34-0440	
CF-1	17.28	17.27 (I_{rel}:90)	0.01		
	19.96	19.97 (I_{rel}:40)	0.01		
	26.52	26.52 (I_{rel}:55)	0		
	28.36	28.4 (I_{rel}:45)	0.04		
	30.08			30.08 (I_{rel}:100)	0
	31.82	31.82 (I_{rel}:80)	0		
	35.66			35.62 (I_{rel}:35)	0.04
	39.22	39.22 (I_{rel}:100)	0		
	44.36	44.39 (I_{rel}:95)	0.03		
	52.48	52.43 (I_{rel}:40)	0.05		
CF-2	17.40	17.27 (I_{rel}:90)	0.13		
	20.12	19.97 (I_{rel}:40)	0.15		
	26.66	26.52 (I_{rel}:55)	0.14		
	28.64	28.4 (I_{rel}:45)	0.24		
	30.06			30.08 (I_{rel}:100)	0.02
	32	31.82 (I_{rel}:80)	0.18		
	35.62			35.62 (I_{rel}:35)	0
	39.50	39.22 (I_{rel}:100)	0.28		
	44.64	44.39 (I_{rel}:95)	0.25		
	52.74	52.43 (I_{rel}:40)	0.31		
CF-3	17.38	17.27 (I_{rel}:90)	0.11		
	20.12	19.97 (I_{rel}:40)	0.15		
	26.68	26.52 (I_{rel}:55)	0.16		
	28.6	28.4 (I_{rel}:45)	0.20		
	30.06			30.08(I_{rel}:100)	0.02
	32.02	31.82 (I_{rel}:80)	0.20		
	35.60			35.62 (I_{rel}:35)	0.02
	39.46	39.22 (I_{rel}:100)	0.24		
	44.60	44.39 (I_{rel}:95)	0.21		
	52.70	52.43 (I_{rel}:40)	0.27		

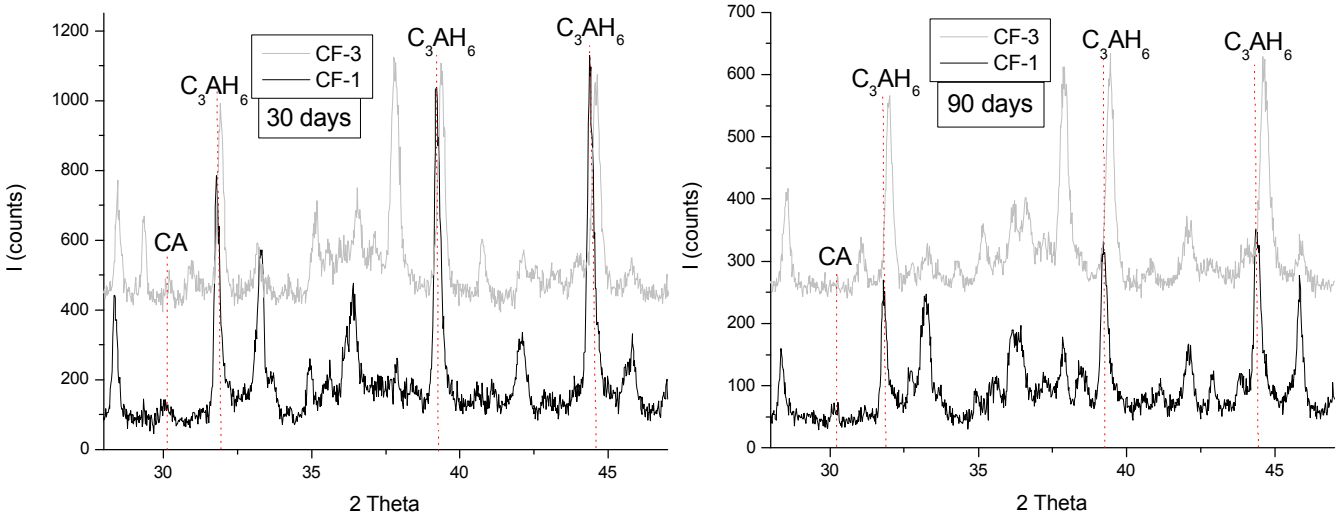

Figure 2. X ray powder diffraction of CF-1 and CF-3 at 30 and 90 days hydration.

3.3 FTIR

FTIR spectrum of fly ash (not shown) presents bands at 3450, 1085, 800, 553 and 465 cm^{-1}. The band appearing at 553 cm^{-1} is associated with the octahedral aluminium present in mullite. Band associated with symmetric stretching vibrations of Si-O-Si (from quartz) and Al-O-Si bonds (tetrahedral aluminium of mullite) appears, however, at 800 cm^{-1}. The bands appearing at around 1170–1130 cm^{-1}, in addition to the T–O vibrations in quartz, are also associated with mullite vibrations. Band appearing at 460 cm^{-1} is associated with O-Si-O or O-Al-O bond bending vibrations.

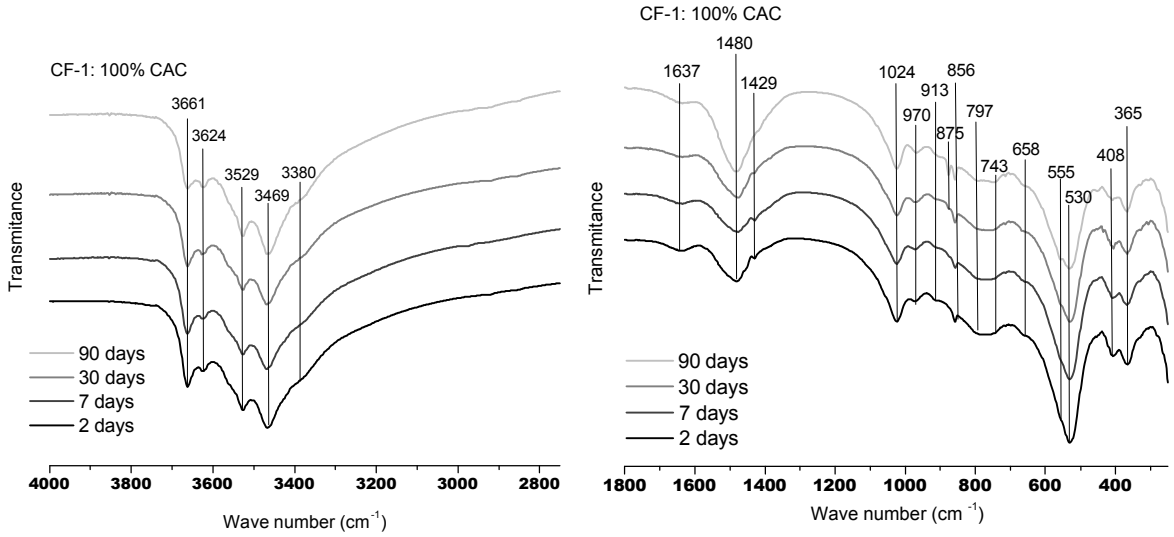

Figure 3. FTIR spectra of CF-1 paste at 2, 7, 30 and 90 days.

Figures 3-5 show the microstructural evolution of CAC and CAC+FA cement based samples. Observing the spectra, gibbsite or aluminium hydroxide seems to be the main solid phase formed. Bands for gibbsite are identified at 3625, 3525, 3472 and 3380 cm^{-1} in the hydroxyl-stretching region. More gibbsite bands were found at 1100, 1025, 970, 948, 915 cm^{-1} and finally low frequency bands at 797, 745, 660, 555, 408 and 365 cm^{-1} [18, 19].

The resolution of gibbsite bands increases for each sample with the reaction time (figures 3-5), indicating an increase on the cristallinity of this phase. However samples including fly ash in the mixture (figures 4 and 5) give less resolved bands indicating the presence of a less crystalline aluminium hydroxide. Infrared shows the loss of cristallinity of gibbsite with the increase in the FA content; an alumina gel is supposed to be formed in these cases. Another possibility is the formation of gibbsite with a lower particle size; it is refereed that decreasing the particle size, the several O-H stretching vibrations at 3500 cm^{-1} merge into a single broad band [18].

Reference sample (CF-1) spectrum shows the 1480 and 856 cm^{-1} absorption peaks, indicating the presence of aragonite as main carbonate polymorph, but the presence of absorption peaks at 1420 and 875 cm^{-1} suggests that calcite is a minor phase.

Hydrated tetracalcium aluminate, $3CaO{\cdot}Al_2O_3{\cdot}CaCO_3{\cdot}11H_2O$ (C_4AcH_{11} using cement chemistry shorthand) was detected at 2 and 7 days of hydration in systems including fly ash on their formulation (see the non overlapped bands at 3676, 1365, 575 and 307 cm^{-1} in figures 4 and 5). The solid solution of hydrogarnet with formula $C_3AS_{3-x}H_{2x}$ appears readily in systems containing monocarboaluminate hydrate at 20°C. In the presence of mineral additions, the calcium carboaluminate hydrate C_4AcH_{11} is formed at the first stages of the hydration process. This specie can be considered as intermediate compound in the hydration process and the precursor of the hydrogarnet $C_3AS_{3-x}H_{2x}$ precipitation. It evolves to a member of the hydrogarnet-garnet solid solution, $C_3AS_{3-x}H_{2x}$ (CASH) and $CaCO_3$ [20].

Systems including fly ash on their formulation show from 7 days of hydration, the transformation of calcium monocarboaluminate hydrate in the CASH member. The transformation can be followed by the disappearing of the band at 3760 cm^{-1} and the appearing of a band at 3660 cm^{-1} assigned to the CASH hydrate, and the disappearing of the band at 1366 cm^{-1} and the strong increase of the intensity of aragonite main band, 1480 cm^{-1} (see figures 4 and 5). In such cases, during the transformation of monocarboaluminate, the introduction of silica on the structure can be favoured. In fact the decomposition of

monocarboaluminate hydrate to gehlenite hydrate in the presence of alite (a source of silica), has been described in the literature [21]. From 7 days hydration time the observed relative intensities of the modes of calcite and the modes of aragonite indicate the presence of aragonite plus a lesser amount of calcite.

Bands in the range 400-500 cm^{-1} are due to deformation of TO_4 tetrahedra (T=Si or Al); the increasing in intensity of this band when the FA content increases is consistent with the formation of a polymerized CASH matrix.

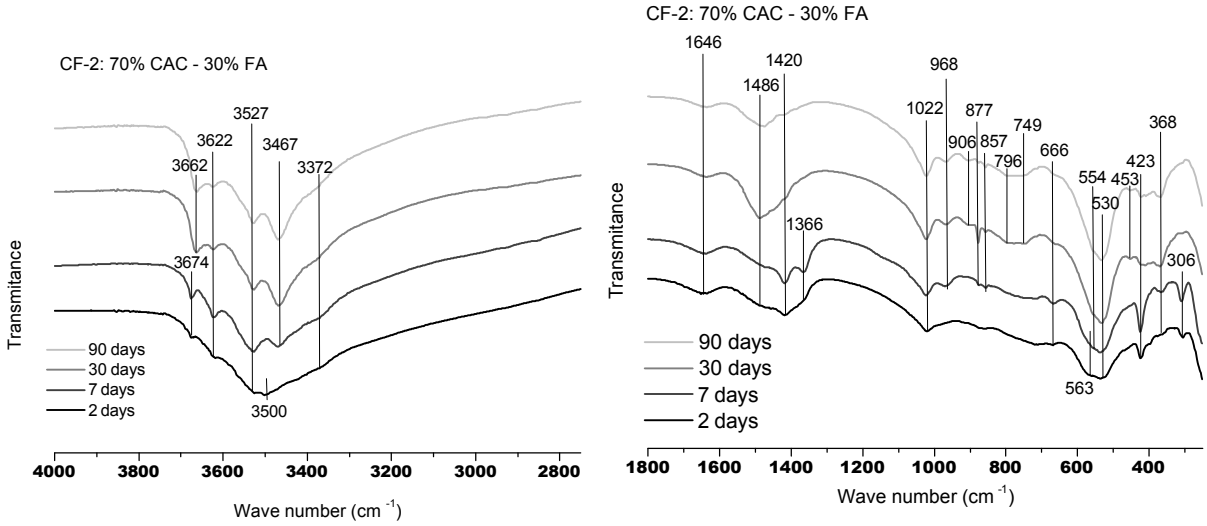

Figure 4. FTIR spectra of CF-2 paste at 2, 7, 30 and 90 days.

The IR spectra of hexagonal hydrates show similarities with each other as might be expected from their common hexagonal plate-type structures [22]; the main difference between cubic hydrates and hexagonal ones is related with the structural formulation $Ca_3[Al(OH)_6]_2$ for cubic hydrogarnet, and the disappearance of the H_2O deformational mode located at 1600 cm^{-1}. However, all hydration products can coexist under these conditions and bands are usually overlapped. According to some authors, main bands of $C_3AS_{3-x}H_{2x}$ solid solution hydrates occur at 3660, 900 and 550 cm^{-1} [23]. These bands appear in CF-1 sample from low reaction times (figure 3), and from 7 days hydration in the case of samples including fly ash on their formulations, fact related with the transformation of calcium monocarboaluminate on a member of the solid solution $C_3AS_{3-x}H_{2x}$.

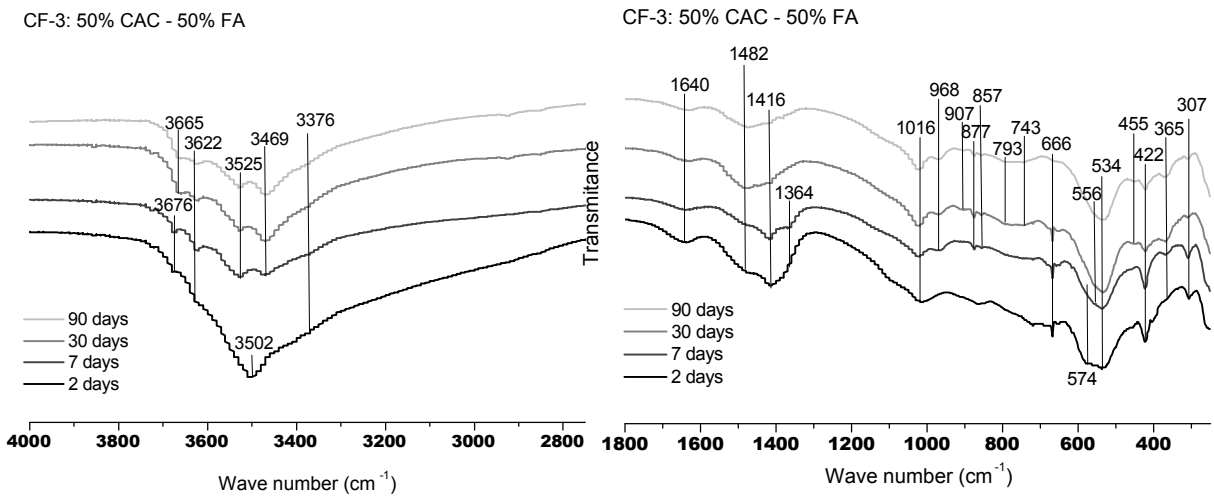

Figure 5. FTIR spectra of CF-3 paste at 2, 7, 30 and 90 days.

4. Conclusions

The effects of the introduction of fly ash on calcium aluminate cement pastes and the phase formation were investigated by XRD, DTA–TGA and FTIR, with the following results:

- Thermal analyses allow identifying a lower content of gibbsite, and a higher content of hexagonal hydrates for samples including fly ash on their formulations. These facts are related with the deceleration of the called conversion reaction.

- The influence of the isomorphous replacement of Al by Si in the hydrogarnet (C_3AH_6) structure is observed in XRD patterns of samples including fly ash, by the shift of measured diffraction peaks. An increase of fly ash content causes an increase of Si/Al ratio in aluminosilicates. The appearance of the grossular end member in sample including 50% of fly ash, induces the neoformation of aluminosilicates such as laumontite and strätlingite.

- The identification of calcium monocarboaluminate in systems CAC+FA at early ages, has been carried out by infrared spectroscopy. Main bands of $C_3AS_{3-x}H_{2x}$ solid solution hydrates occur at 3660, 900 and 550 cm^{-1}. Modes of comparable intensity and frequency were observed for all samples, but for CAC+FA mixes they appear after 7 days of hydration. This fact was related with the transformation of calcium monocarboaluminate on a member of the solid solution $C_3AS_{3-x}H_{2x}$ and $CaCO_3$.

5. Acknowledgments

The financial support of ESDRED EC project: "Engineering Studies and Demonstration of Repository Designs", the Spanish waste national management agency “ENRESA” and Région Poitou-Charentes (Convention 04/RPC-R-120) is greatly acknowledged.

References

[1] H.G. Midgley, A. Midgley, The Conversion of High Alumina Cement, Mag. Concr. Res. 27, (1975) 59-77

[2] A. Capmas C.M. George, Durability of Calcium Aluminate Cement Concretes, Advances in Cement and Concrete Res, Proc. Of Engineering Foundation Conf., Durham, N.H., Materials Engineering Division, ASCE, (1994) 377-405

[3] M.N. Grutzeck and S. L. Sarkar, Editors, Proc. Eng. Foundation Conf. (July 24-29, 1994). New Hampshire, Publ. Amer. Soc. of Civil Eng. NY

[4] C. Del Olmo, Revista Iberoamericana de Corrosión y Protección, April, 201 (1976)

[5] T. Vázquez, F. Triviño and A. Ruiz de Gauna, Monography at the Eduardo Torroja Institute, IccET, Nº 334 (1976)

[6] A.J. Majumdar, B. Singh, R.N. Edmonds, Hydration of Secar 71 aluminous cement in presence of granulated blast furnace slag . Cement and Concrete Research, 20, (1990) 7-14.

[7] A.J. Majumdar, B. Singh, R.N. Edmonds, Hydration of mixtures of “ciment fondu” aluminous cement and granulated blast furnace slag . Cement and Concrete Research, 20, (1990) 197-208.

[8] K. Quillin, G. Osborne, A. Majumdar, B. Singh, Effects of w/c ratio and curing conditions on strength development in BRECEM concretes. Cement and Concrete Research, 31 (2001) 627-632.

[9] J. Ding, Y. Fu, J.J. Beaudoin, Strätlingite formation in high alumina cement-silica fume systems: significance of sodium ions. Cement and Concrete Research, 25 (1995) 1311-1319.

[10] A.J. Majumdar, B. Singh, Properties of some blended high-alumina cements . Cement and Concrete Research, 22 (1992) 1101-1114.

[11] A.J. Majumdar, R.N. Edmonds, B. Singh, Hydration of calcium aluminate in presence of granulated blast furnace slag, Calcium Aluminate Cement, Proc. Inter. Sym. Queen Mary and Westfield College, University of London, 9-11 July, Chapman and Hall, London, (1990) p.259.

[12] M. Collepardi, S. Monosi, P. Piccioli, The influence of pozzolanic materials on the mechanical stability of aluminous cement. Cement and Concrete Research, 25 (1995) 961-968.

[13] J.M. Rivas Mercury, X. Turrillas, A.H. de Aza, P. Pena, Calcium aluminates hydration in presence of amorphous SiO_2 at temperatures below 90ºC. Journal of Solid State Chemistry 179 (2006) 2988-2997

[14] R.C. Mackenzie, Differential Thermal Analysis, Academic Press, London and New York, 1970

[15] J.M. Rivas Mercury, A.H. de Aza, X. Turrillas, P. Pena, Hidratación de los cementos de aluminatos de calcio. Parte II: efecto de las adiciones de sílice y alumina. Bol. Soc. Esp. Ceram. V., 42 [6] (2003) 361-368

[16] R.N. Edmonds, A.J. Majumdar, The hydration of 12CaO·7Al2O3 at different temperatures. Cement and Concrete Research, 18 (1988) 473-478.

[17] B. Singh, A.J. Majumdar, K. Quillin, Properties of BRECEM. Ten-year results. Cement and Concrete Research, 29 (1999) 429-433.

[18] R. L. Frost, J. Kloprogge, S.C. Russell, J.L. Szetu, Dehydroxylation and structure of alumina gels prepared from trisecbutoxyaluminium, Thermochimica Acta, 329(1999) 47-56.

[19] J.A. Gadsden, Infrared spectra of minerals and related inorganic compounds, Butterworths, London, 1975.

[20] G. Renaudin, M. Francois, O. Evrard, Order and disorder in the lamellar hydrated tetracalcium monocarboaluminate compound. Cement and Concrete Research, 29 (1999) 63-69.

[21] H.Y. Ghorab, E.A. Kisbar, S.H. Abou Elfetouh, Studies on the stability of the calcium sulfoaluminate hydrates, Part III: the monophases. Cement and Concrete Research, 28 (1998) 763-771.

[22] M.A. Trezza, A.E. Lavat, Analysis of the system $3CaO·Al_2O_3$-$CaSO_4·2H_2O$-$CaCO_3$-H_2O by FT-IR spectroscopy, Cement and Concrete Research, 31 (2001) 869-872

[23] S. Fujita, K. Suzuki, Y. Shibasaki, T. Mori, Synthesis of hydrogarnet from molten slag and its hydrogen chloride fixation performance at high temperature, J Mater Cycles Waste Manag 4 (2002) 70-76